Effect of Amphiphile Size on the Transformation from a Lyotropic Gel to a Vesicular Dispersion

Giuseppe Battaglia* and Anthony J. Ryan*

Department of Chemistry, University of Sheffield, Sheffield S3 7HF, UK

Received September 28, 2005; Revised Manuscript Received November 15, 2005

ABSTRACT: The sequence of phases formed by amphiphilic copolymers on dilution in water has been studied for two poly(ethylene oxide)-*co*-poly(butylene oxide) copolymers with the same hydrophobe−hydrophile ratio but different molecular weights. The size of the amphiphile significantly affects both the formation of lyotropic phase and dispersed vesicles. The evolution from the bulk solid to lyotropic liquid shows that the low molecular weight copolymer assembles first into an inverted hexagonal structure and then lamellae, whereas the high molecular weight dissolves directly to the lamellar phase. The transition from lamellae to the sponge phase is essentially unaffected by the molecular weight of the amphiphiles. In contrast, however, the evolution of the sponge phase into vesicles is qualitatively different depending on the size of the amphiphile. The smaller amphiphile forms dispersed vesicles at quite high concentrations, whereas the high molecular weight polymer initially forms peculiar vesicular gel clusters, which eventually break up into dispersed vesicles. The amphiphile size also has a particular effect on the nature of the vesicles formed, the larger amphiphile forms uniquely unilamellar vesicles on dilution whereas the smaller amphiphiles make multilamellar vesicles while still in a lyotropic solution. Obviously, membrane undulations and membrane unbinding depend strongly on the stiffness of the amphiphilic membrane, which is dominated by the size. More flexible membranes lead to earlier unbinding and multilamellar vesicles, and as membrane flexibility is reduced unbinding occurs at lower concentrations and unilamellar vesicles result.

Introduction

Amphiphiles are bipolar molecules made of hydrophilic segments chemically attached to hydrophobic segments. Once dissolved in water, these twofold compounds self-assemble into nanoscopic structures. The architecture of such supramolecular aggregates is governed by the delicate balance between attractive forces and repulsive forces arising from the interactions between water and the respective hydrophilic and hydrophobic segments.[1,2] On the basis of simple geometrical considerations, highly hydrophilic molecules assemble into spherical micelles, and as the amphiphiles become more hydrophobic, cylindrical micelles and eventually amphiphilic membranes will result from the balance of hydrophilic and hydrophobic interactions. These simple structures are known as normal structures and at low concentrations are singularly dispersed, but as the water content decreases, the normal structures undergo to a secondary self-assembly generating lyotropic phases, also known as liquid crystals, whose morphology has long-range order.[3]

This remarkable behavior, initially discovered in small molecules such as lipids and detergents, has been also reported for higher molecular weight systems such as amphiphilic block copolymers. Their macromolecular nature confers greater stability and enhances the mechanical properties to the final supramolecular aggregates.[4] Several examples of polymeric micelles and vesicles have been reported.[5−11] In particular, the latter structures have been gaining more attention as they reassemble those generated by biological membranes in cellular compartmentation and therefore offer outstanding possibilities to design nanocontainers that can find applications in biomedicine[12,13] and electronics.[14]

While micelle-forming block copolymers have been extensively characterized,[15−18] the behavior of vesicles-forming copolymers in water is not yet fully understood. Since polymeric vesicles are gaining attention in the scientific community and in diverse applications such as cosmetics, food formulations, and drug delivery systems, it is important to understand the assembly of such macromolecules as a function of their concentration in water, particularly as commercial formulations are often made by dissolving dry amphiphile. From studies on small amphiphiles,[19−22] membranes are known to undergo morphological transitions through a sequence of intermediate phases upon dilution in water. The vesicle formation process occurs by diffusion of water into a concentrated polymer film setting up a concentration gradient that contains the full phase sequence. At high concentration, the most stable structures are lamellar stacks, whose periodicity increases as the water content increases. This phenomenon, known as lamellar swelling, is linear with concentration up to a point where the repulsive interactions overcome the attractive interaction and the lamellar sheets start to unbind. At this point the membranes ought to reassemble into structures that avoid the contact between the hydrophobic membrane and the water. One possible route is the formation of dispersed unilamellar and multilamellar vesicles;[21,23] however, in many cases, after the membranes are unbound, the amphiphile−water system still has the consistency of a gel indicating the presence of a lyotropic phase. One geometry that satisfies the conditions containing unbound membranes and being highly viscoelastic is the sponge phase.[24,25] This bicontinuous structure is made of channels of water surrounded by amphiphilic membranes and is the most likely geometry generated as consequence of the membrane unbinding.

The membrane unbinding process has been extensively studied, both theoretically[26−28] and experimentally,[23,26] and been found to be dependent on thermal fluctuations of the membranes. The magnitude of such fluctuations depends on the molecular properties of the membrane, particularly the stiffness, and will determine the ultimate fate of the unbound membranes, that is, whether unbinding will proceed via the formation of a sponge phase, multilamellar vesicles, or unilamellar vesicles.

* Corresponding authors. E-mail: g.battaglia@shef.ac.uk, tony.ryan@shef.ac.uk.

10.1021/ma052108a CCC: $33.50
Published on Web 12/20/2005

In the case of amphiphilic block copolymers, the membrane has been found to be very stiff,[4,29] a result of entangled[5] hydrophobic chains, and in contrast to the very mobile, small amphiphile membranes. This feature will, of course, affect the sequence of phase transitions upon dilution in water. In a recent study[30] the phase sequence of a vesicle forming poly(ethylene-oxide)-*co*-poly(butylene oxide) ($E_{115}B_{103}$) has been studied as a function of water content. Three different transitions were identified—lamellae—sponge—hexagonally packed vesicles—dispersed vesicles—showing that these stiffer amphiphilic membranes can still rearrange to accommodate increases in water content.

Here we study membrane arrangement upon dissolution in water comparing a lower molecular weight block copolymer $E_{16}B_{22}$ (M_w = 2.3 kg mol^{-1}) to that previously reported[30] $E_{115}B_{103}$ (M_w = 12 kg mol^{-1}). Both polymers can form unilamellar vesicles[5] with membrane thicknesses of 2.4 and 7.4 nm, respectively; $E_{16}B_{22}$ is a homogeneous liquid in the bulk whereas $E_{115}B_{103}$ is a semicrystalline lamellar solid that melts to form a microphase-separated structure of E-rods in a B matrix.[31,33]

Experimental Section

Materials. Copolymers were prepared by sequential anionic copolymerization and were characterized using gel permeation chromatography and ^{13}C NMR spectroscopy as described elsewhere.[15,31]

Dynamic Light Scattering. Measurements were performed on a Brookhaven Instruments 200SM laser light scattering goniometer using a He−Ne 125 mW 633 nm laser. The vesicle dispersions are placed into glass vials. Single scans of 10 min exposure were performed on the sample. Particle sizes were estimated using the nonnegative least-squares (NNLS) multiple pass method of data analysis.

Small-Angle X-ray Scattering. Copolymers were dissolved in water at different concentrations. The samples were sealed and kept, when liquid, under stirring for 3 weeks. Small-angle X-ray scattering experiments were performed using a Bruker AXS Nanostar equipped with a Cu Kα X-ray source at wavelength λ = 1.54 Å and a camera length of 1.05 m, with a data collection time of 9 h. Low-concentration samples were analyzed on beamline 6.2 of the Synchrotron Radiation Source (SRS) at the Daresbury Laboratory, Warrington, U.K. The beamline is configured for SAXS experiments using monochromatic radiation of wavelength[32] λ = 1.4 Å, and data were collected for 5 min. All the SAXS patterns shown have been corrected for background scattering and the scattering from water according to their concentration.

Transmission Electron Microscopy. The copolymer−water mixtures were engrossed on precoated in carbon copper grids. The grids are submerged for 20 s into the sample solution and then in uranyl acetate water solution (2% w/w). Imaging was performed on a Philips CM100 instrument equipped with a Gatan 1k CCD camera.

Results and Discussion

Lyotropic Phases. Solid high molecular weight E−B copolymers such as the $E_{115}B_{103}$ have been observed[30,31] to be microphase-separated, semicrystalline solids at room temperature and generally have a lamellar structure, as can be seen in Figure 1b. $E_{16}B_{22}$ is a very viscous liquid at room temperature, and the scattering pattern in Figure 1a shows a weak maximum associated with density fluctuations and the correlation typical of block copolymers above the order−disorder temperature.[31]

Figure 2 presents SAXS pattern of both $E_{16}B_{22}$ and $E_{115}B_{103}$ as a function of concentration. The low molecular weight copolymer, once mixed with water, has an enhanced segregation between hydrophilic and hydrophobic blocks. A swollen ordered hexagonal phase, made of cylindrical aqueous PEO rods surrounded by a continuous hydrophobic phase, can be observed

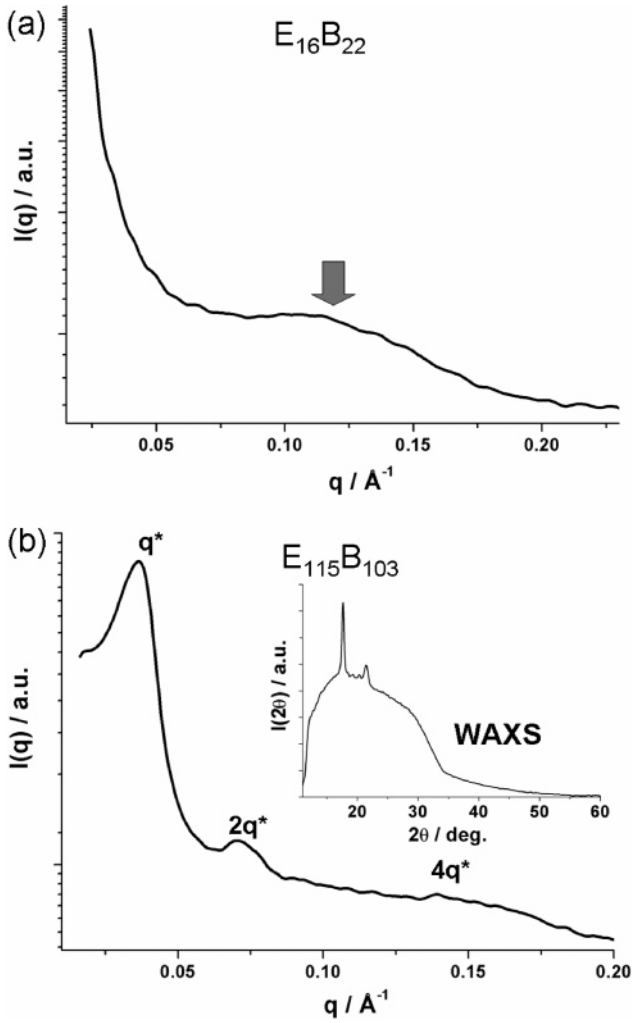

Figure 1. (a) 1D SAXS pattern of dry $E_{16}B_{22}$. The presence of very broad peak is the scattering from composition fluctuations typical of block copolymers below their order−disorder temperature. **(**b**)** 1D SAXS and 1D WAXS patterns of dry $E_{115}B_{103}$.The location of the expected reflection at q^* is in this copolymer at $2q^*$, and $4q^*$ indicating a lamellar morphology; the WAXS pattern confirms the semicrystalline nature of the block copolymer, indicating that the lamellae are made by the periodic arrangement of crystalline PEO and amorphous PBO layers.

at concentrations between 90 and 70% w/w water. $E_{16}B_{22}$ forms the hexagonal phase expected from the phase volumes and the bulk block copolymer phase diagram. The larger $E_{115}B_{103}$ dissolves directly into a lamellar phase at high concentration, which is in contrast to its behavior in the bulk, which has a hexagonal phase[31,33] on melting, and the behavior of the smaller homologue. $E_{115}B_{103}$ is lamellar when dry at room temperature, and the water addition can be thought as a melting the crystalline PEO. The data presented in Figure 2 clearly reveal the formation of well-ordered lyotropic lamellae at 90% w/w in water, and the lamellae show the expected linear scaling with dilution. It could be that at very high concentrations (i.e., close to 100%) the systems might produce a hexagonal arrangement, and this is currently being tested. The $E_{115}B_{103}$ is lamellar when dry, however, and this may affect the subsequent phase formation, that is, the copolymers are already organized into layers, and the formation of a layered phase, by dissolution melting, is energetically more favorable than the formation of discrete rods. Moreover, the hexagonal geometry in the melt is a result of interactions between the two blocks whereas in the solution it is the ternary interaction of water and the two blocks. It has been reported[5] previously that the hydrated E−B χ coefficient

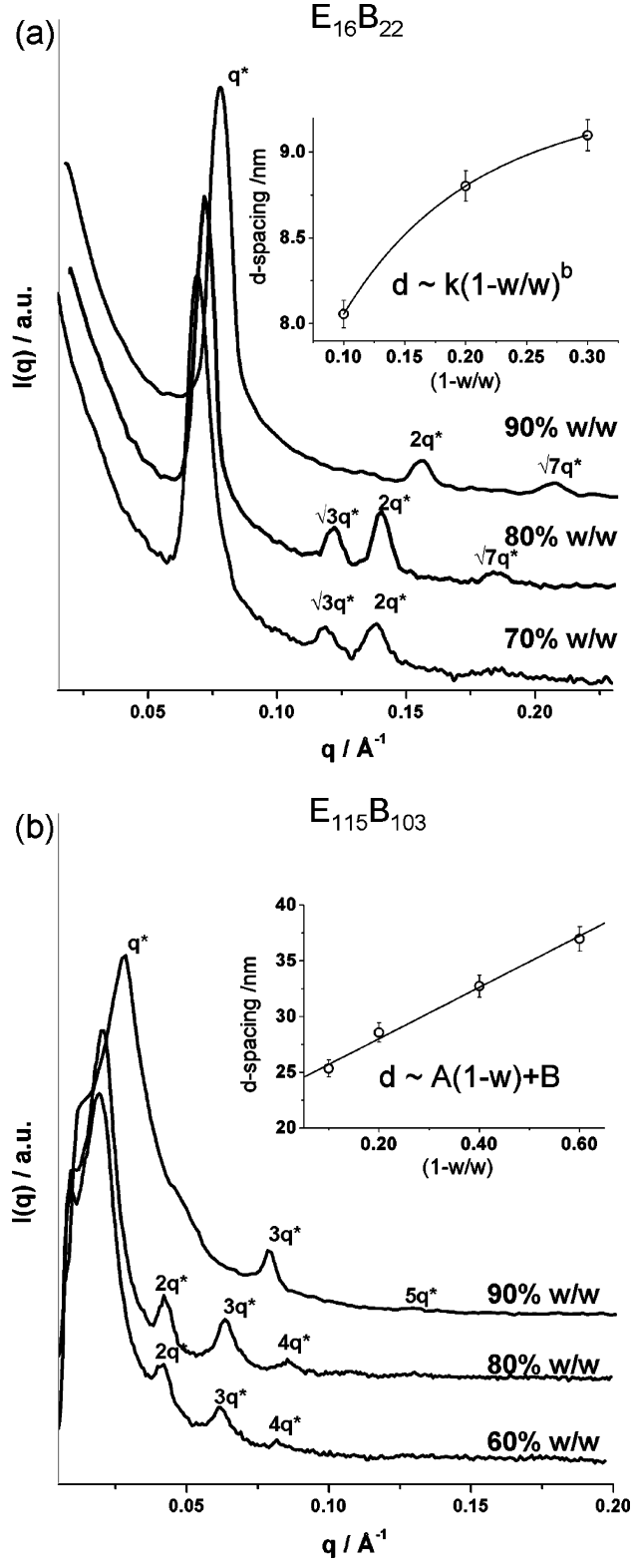

Figure 2. **(a)** SAXS patterns from aqueous solutions of 90, 80, and 70% w/w $E_{16}B_{22}$. A well-ordered hexagonal phase of aqueous PEO rods surrounded by a continuous PBO phase. The location of the expected reflection at q^*,$\sqrt{3}q^*$, $\sqrt{4}q^*$, and $\sqrt{7}q^*$ are marked. In the 90% solution the $\sqrt{3}q^*$ reflection is systematically absent due to its coincidence with the minimum in the form factor of the cylinders. The *d* spacing of the hexagonal rods increases as the water content increases; the swelling follows a power law typical of inverted hexagonal phases. **(**b**)** SAXS patterns from aqueous solutions of 90, 80, and 60% w/w $E_{115}B_{103}$. The location of the expected reflection at q^* are in this copolymer at $2q^*$, $3q^*$, and $4q^*$, indicating a lamellar morphology. The *d* spacing increases linearly as the water content increases, in agreement with the lamellar morphology.

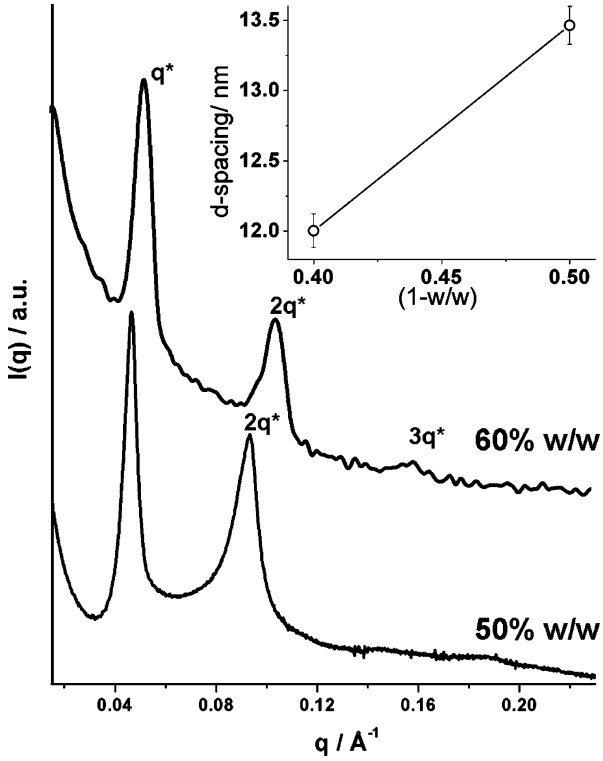

Figure 3. SAXS patterns from aqueous solutions of 60 and 50% w/w $E_{16}B_{22}$. A well-ordered lyotropic lamellar is formed, and the locations of the expected higher-order reflection at $2q^*$ and $3q^*$ are marked. In the inset the lamellae swelling is represented as *d* spacing vs water content.

is bigger than that of bulk EB, and the lamellar phase is known to be more stable (i.e., exist over a wider composition range) at higher χN.

When $E_{16}B_{22}$ first contacts water, it has no order and its liquid nature makes its chains more mobile. It can be that the water−PBO chain interactions are overcome by the interactions between PEO and PBO. The interfacial energy between the blocks is increased by the addition of water and in this drives the formation of a hexagonal phase from a fluctuating structure.

At concentrations between 70% and 60% the hexagonal phase of $E_{16}B_{22}$ transforms into a lamellar phase (Figure 3). This confirms a strong concentration dependence of the interactions between the amphiphilic block copolymer and the water.

Membrane Unbinding. At high amphiphile concentrations in water attraction forces dominates, and the membranes are in a bound state, with the lamellae *d* spacing being determined by the position of the minimum in the interaction potential. The *d* spacing increases as the water content increases up to point where the repulsive forces overwhelm the attractive interaction. The minimum in the interaction potential would then vanish, and the system would transform from a bound to an unbound state.

There have been several theoretical studies of the unbinding transition, and it has been predicted to be continuous in the case of two interacting membranes, with the bilayer separation diverging at the transition. However, scaling arguments have indicated that the width of the critical region is inversely proportional to the number of membranes in a stack, and therefore, for a multimembrane system, the unbinding transition is expected to appear discontinuous.[26] Furthermore, on the basis of membrane bending energy,[34] membrane undulations are expected to induce a characteristic repulsion due to the excluded-volume effect, so-called "Helfrich repulsion". Anyhow, an unbinding transition results in a remarkable change of the lamel-

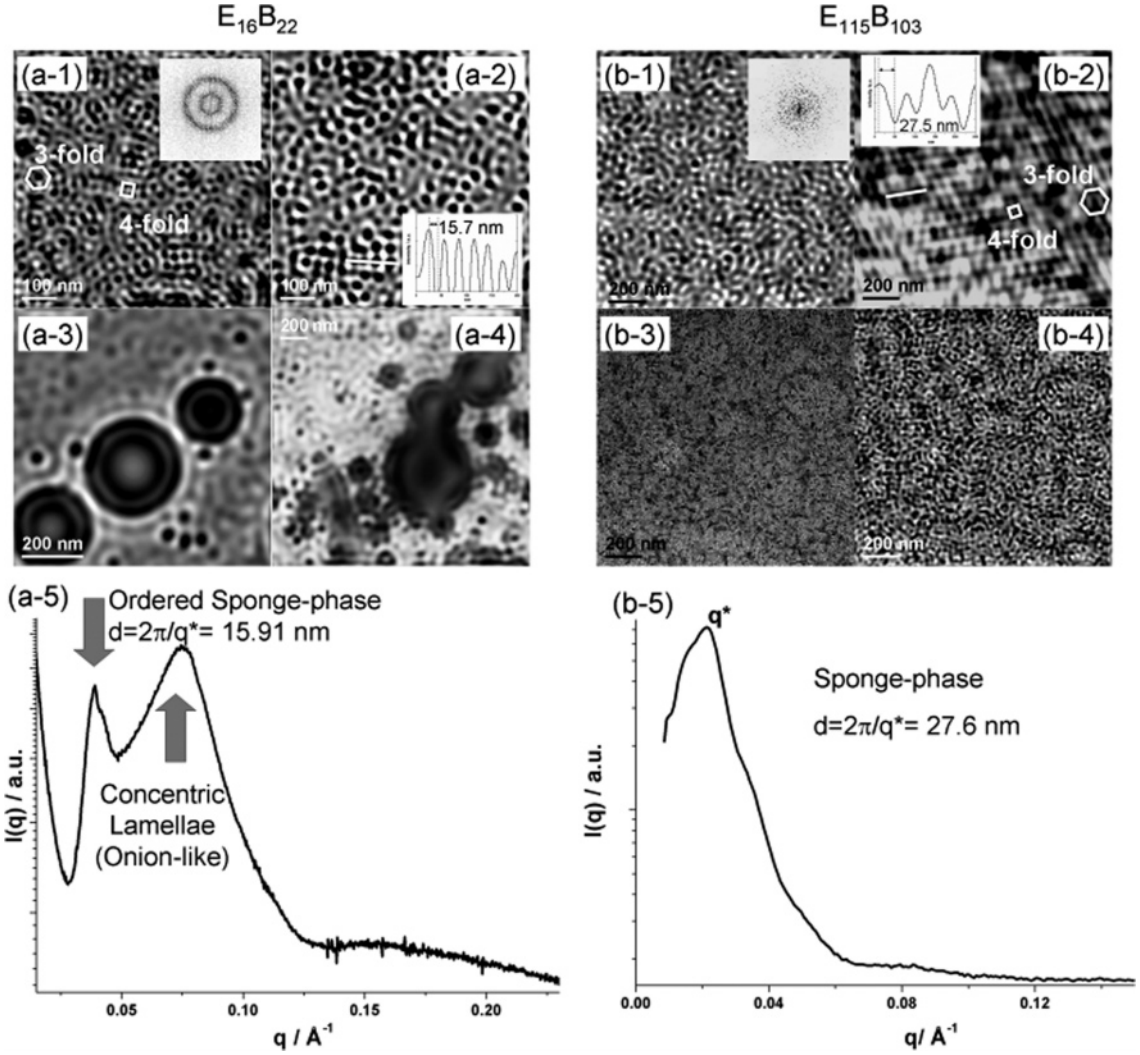

Figure 4. **(**a-1, a-2**)** TEM micrographs of negative stained $E_{16}B_{22}$ at a concentration in water of 40% w/w. $E_{16}B_{22}$ has a sponge structure; the presence of both 3- and 4-fold symmetry and the Fourier transform indicate a bicontinuous cubic structure. Together with the sponge phase there is a noticeable coexistence of multilamellar vesicles **(**a-3**)** and **(**a-4**)**. **(**a-5**)** Signatures of both structures appear also in the 1D SAXS pattern; the *d* spacing calculated from the *q** has a good match with the periodicity measured by TEM. (b-1, b-2, b-3, and b-4**)** TEM micrographs of negative stained $E_{115}B_{103}$ at concentration in water of 30% w/w. The higher molecular weight copolymer also shows sponge bicontinuous cubic structure. **(**b-5**)** SAXS pattern of the same copolymer−water mixture shows the presence one peak whose periodicity matches the value calculated by TEM.

lar structure[35] in an amphiphile−water mixture, and the final morphology depends on how the membrane undulations evolve.

At 40% w/w of $E_{16}B_{22}$ and 30% w/w of $E_{115}B_{103}$ in water we observe the loss of the lamellar morphology and a new phase, that we suggest is the result of the membrane unbinding, has been found. TEM analyses (Figures 4a-1, 4a-2, 4b-1, 4b-2, 4b-3, and 4b-4) have revealed the presence of a sponge phase with channels arranged with long-range order. TEM micrographs show that such arrangement is cubic, as both 3-fold and 4-fold symmetries can be observed; the sponge phase has a bicontinuous cubic structure, and in some cases there is sufficient long-range order that the crystallographic arrangement can be defined as *Im*3*m*.

TEM have also shown (Figures 4a-3 and 4a-4) the substantial coexistence of concentric multilamellar domains that are often referred to as onions.[36] SAXS analyses (Figure 4a-5) performed on the same sample have shown the presence of two peaks which are the result of two separately scattering systems. The first peak is rather sharp whereas the second is more intense but diffuse. There is a minimum in the scattering around $q \sim 0.125$ Å that is characteristic of membrane thickness of 2.5 nm. The scattering pattern is, therefore, the sum of two different structure factors: the ordered sponge phase and the concentric lamellae, with a common form factor from the fundamental building block of the interdigitated membrane. TEM measurements of the periodicity of the bicontinuous cubic structure match the *d* spacing calculated from the SAXS peak with $d = 15.4$ nm (Figures 4a-2 and 4a-5). The high molecular weight material does not show any multilamellar vesicles, and its SAXS pattern is just the result of the sponge-phase structure (Figure 4b-5); once again TEM and SAXS measurements are in good

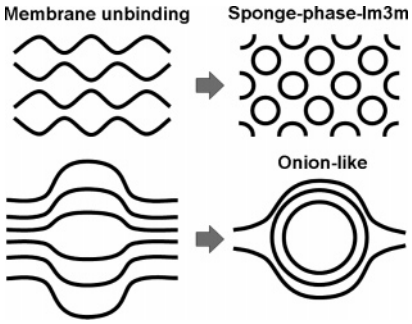

Figure 5. Proposed mechanism of membrane undulations as consequence of the direct observation of the morphology after the lamellae unbinding.

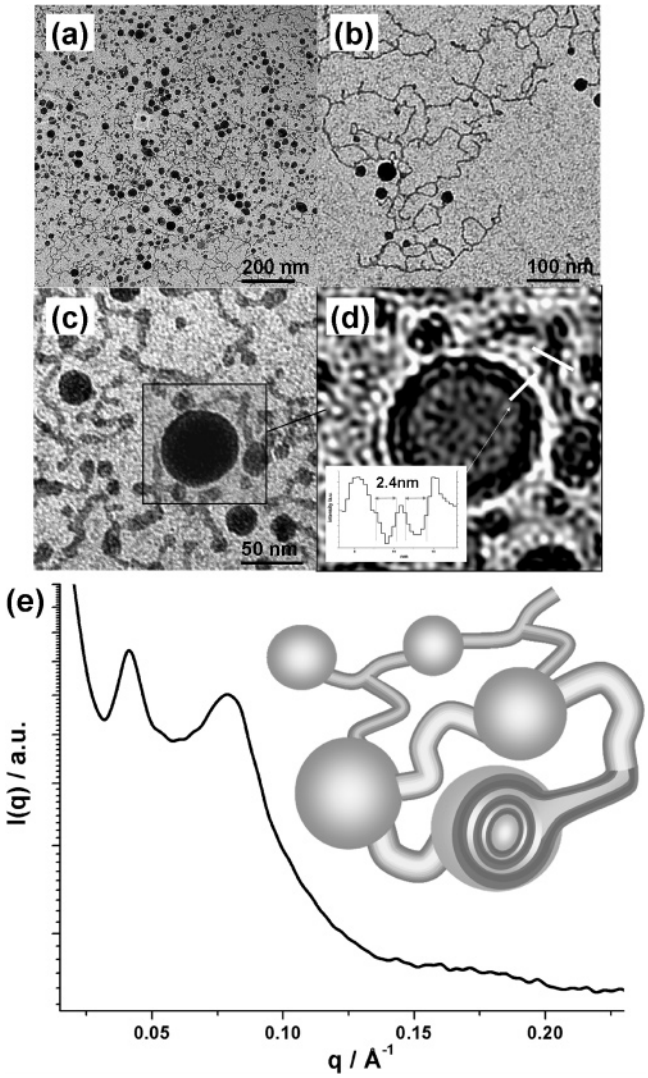

Figure 6. **(**a−d**)** TEM micrographs of negative stained $E_{16}B_{22}$ at concentration in water of 20% w/w. The $E_{16}B_{22}$−water assembly structure has the morphology of gel made of multilamellar vesicle interconnected by lamellar tubules. **(e)** 1D SAXS pattern of the same concentration mixture has the characteristics two form factors arising from the spherical vesicles and the lamellar tubules.

agreement (Figures 4b-2 and 4b-5). In a previous study, Alexandridis et al.[37] found that another EB diblock copolymer, with the same composition but a different molecular weight, also transformed to a sponge phase at same concentration of 30% w/w in water. Its structure was resolved, showing that it is symmetrical and has a periodic minimal surface known as the P-surface[38] with an *Im*3*m* crystallographic arrangement of interfaces.

The two-phase morphology observed at 40% w/w in the $E_{16}B_{22}$ suggests that the membrane undulations might evolve according two different periodicities (Figure 5). The sponge *Im*3*m* seems to be the result of periodic modulations with short wavelength, which are in counterphase with the next layer. Such types of membrane undulations were previously reported as "egg-carton structure" resulting from Monte Carlo simulations based on bending elasticity calculations.[28] Conversely, the onionlike structures suggest the presence of giant correlated fluctuations[21] that are in counterphase with the next three or four layers. Both undulations will eventually trigger the membrane fusion in the contacts points and therefore the transition of lamellae to sponge phase.

Lyotropic−Isotropic Transition: Vesicular Gels and Dispersed Vesicles. The sponge phase is still observable down to 30% w/w for $E_{16}B_{22}$ and 20% w/w/ for the $E_{115}B_{103}$ with very little difference in terms of morphology and *d* spacing. At 20% w/w in water, the $E_{16}B_{22}$−water still has the consistency of a gel, and SAXS analysis (Figure 6e) does not show any presence of the sponge phase; instead, 20% w/w $E_{16}B_{22}$−water seems to have a pattern which results from two independently scattering structures. The second peak has the same position and shape as the peak associated with the form factor of multilamellar vesicles as in Figure 4e, whereas the first peak might be associated with a structural peak of the sponge phase or the form factor of some other morphology. Such complex morphology has been disclosed by TEM observations. The three TEM micrographs in Figure 6a−c show the structure of random network made of multilamellar vesicles (onionlike) connected via lamellar tubules. Both the tubule membrane and the multilamellar vesicles membranes have been measured a thickness of 2.4 nm (Figure 6d). The same value was observed for unilamellar vesicles made from this polymer and reported in a previous work.[5] This peculiar geometry seems to suggest that the sponge phase in Figure 4 evolves as the water content increases by losing the order and the periodicity of the sponge phase. The water channels that made the bicontinuous cubic phase are now stretched over a few hundred nanometers as lamellar tubules connecting the multilamellar vesicles observed at higher concentrations. These micrographs therefore indicate that the SAXS pattern seems to be the result of two different form factors (the multilamellar vesicle and the lamellar tubules), and no structural peaks are present.

Around 10% w/w of $E_{16}B_{22}$ in water, the mixture turns from gel to turbid liquid. Both SAXS and TEM analysis have revealed that the liquid comprises a dispersion of both multilamellar and unilamellar. This morphology is maintained of dilution below 10% copolymer. The micrographs in parts a, b, and c of Figure 7 at 10%, 5%, and 1% w/w, respectively, show the coexistence of both multilamellar and unilamellar vesicles. Apart from the vesicle number density, all the samples are structurally similar. Scattering experiments confirmed such results as all the liquid samples have typical SAXS pattern of vesicle dispersion (Figure 7d) with a form factor associated with lamellae. The multilamellar vesicles are those that were already present at high concentration connected to the sponge phase. At 20% they were connected by lamellar tubules; now it appears that the precursor bicontinuous channels and the lamellar tubules have also transformed into unilamellar vesicles.

In this concentration regime the high molecular weight $E_{115}B_{103}$ follows a different structural evolution. Instead of dispersed vesicles, the sponge phase breaks up into gel clusters made of the almost regular packing of unilamellar vesicles (Figure 8a,b). Only at concentration around 1% w/w do the clusters eventually break up into dispersed vesicles (Figure 8c). This phenomenon can also be observed by SAXS (Figure 8d) as the ordered structure of the gel cluster can be confirmed by the presence of a quite intense structural peak. At higher concentration the first peak at 32 nm arises from the hexagonal-close packing[30] of vesicles and is confirmed by the shoulder at $\sqrt{3}q^*$. Once the vesicles disperse, no structural peak can be observed. At this molecular weight, also in the dispersed phase, almost no multilamellar vesicles have been observed.

In the $E_{16}B_{22}$ both unilamellar and multilamellar vesicles are still observable in very dilute concentrations; however, the only structural analysis that can be performed is dynamic light scattering (DLS). Particles size analyses (Figure

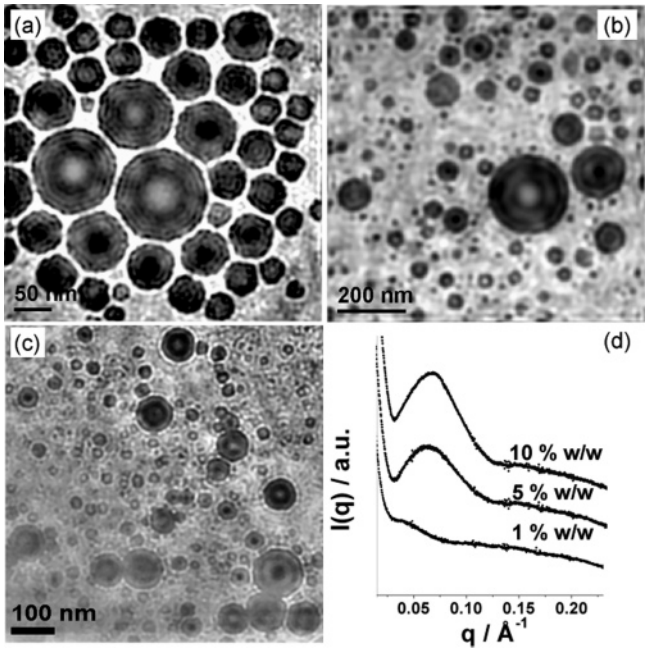

Figure 7. **(**a**)**. TEM micrographs of negative stained $E_{16}B_{22}$ at concentration in water of 10% w/w, **(**b**)** 5% w/w, and **(**c**)** 1% w/w. All the three samples have showed the presence of multilamellar and unilamellar vesicles. **(**d**)** 1D SAXS patterns of the same concentrations show again typical characteristics of dispersed vesicles.

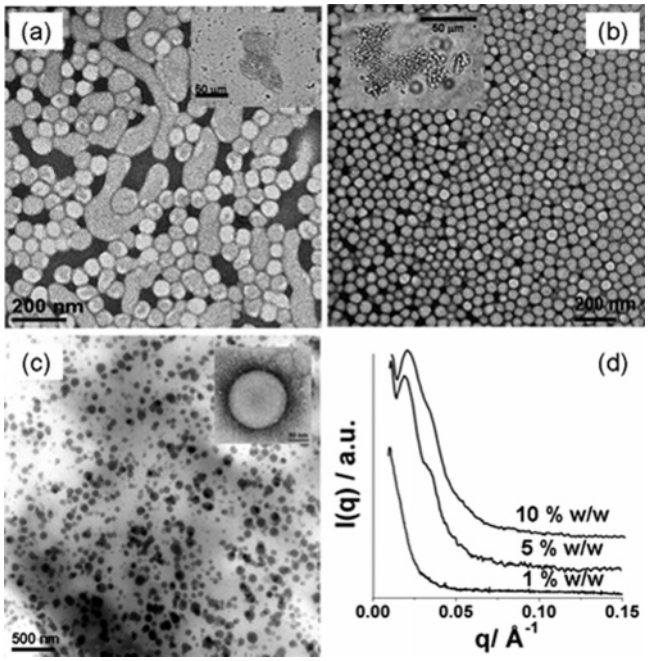

Figure 8. **(**a**)** TEM micrographs of negative stained $E_{115}B_{103}$ at concentration in water of 10% w/w, **(**b**)** 5% w/w, and **(**c**)** 1% w/w. As already reported previously,[30] the evolution of vesicles in this specific block copolymer occur via the formation of gel clusters made of the packing of vesicles. Eventually at low concentration these cluster breaks up in dispersed vesicles. **(**d**)** 1D SAXS patterns of the same concentrations show that liquid samples at concentration between 10 and 5% w/w have still a peak due the structural arrangement in the gel clusters; at 1% w/w, no structural peak is present, indicating the copolymer is assembled into dispersed vesicles.

9) performed on different correlation functions have showed a bimodal distribution, indicating a dispersion made of two different populations: one with diameter around 1 μm and another one around 100−200 nm. On the basis of the previous results and especially the TEM micrographs in Figure 7a−c, we suggest that the two different populations are respectively

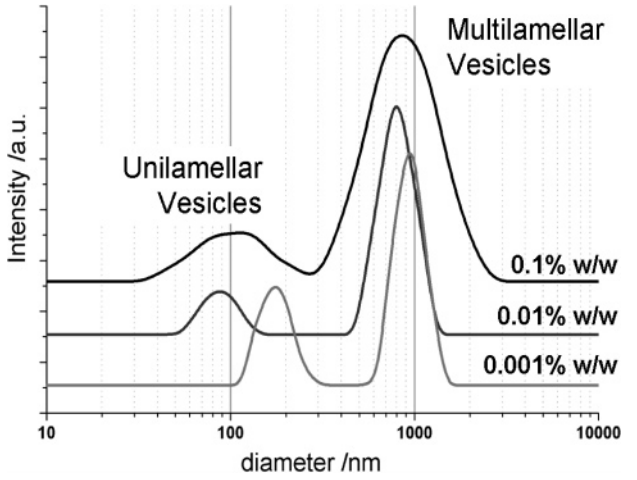

Figure 9. Particle size distributions of $E_{16}B_{22}$ at concentrations in water of 0.1, 0.01 and 0.001% w/w. The bimodal distribution is the result of the coexistence of multilamellar and unilamellar vesicles. The size distributions show some changes as effect of the concentration. Both populations get more monodisperse, and the amount of unilamellar vesicles seems to increase.

the multilamellar vesicles and the unilamellar vesicles. DLS measurements have also shown that both populations become less polydisperse as the concentrations decreases and the peak corresponding to the unilamellar vesicles grows as the concentration decreases, indicating that multilamellar vesicles transform into unilamellar vesicles. This result implies that multilamellar vesicles are more a metastable phase and the result of defects in the original lamellar structure. Indeed, when extruded or sonicated all the multilamellar vesicles disappear as previously[5] demonstrated for this amphiphilic block copolymer.

Conclusions

All the results presented herein, and the results from ref 30 can allow us to map an isothermal plane of the molecular weight vs concentration phase diagram of E_mB_n and water where the amphiphile contains a hydrophobic fraction of around 0.7 (see Figure 10).

The phase behavior of membrane-forming E_mB_n copolymers in water strongly depends on both concentration and molecular weight. The effects of the very initial hydration on the copolymer are remarkably different as a function of the molecular weight: the low molecular weight $E_{16}B_{22}$ generates a hexagonal phase made of cylindrical aqueous E rods surrounded by a continuous hydrophobic B phase, whereas the higher molecular weight $E_{115}B_{103}$ forms a lamellar phase directly. This substantial difference can be understood on the basis of different interfacial energies between aqueous E and B compared with bulk E/B. The hexagonal geometry in the melt is a result of interactions between the two blocks whereas in the solution it is the ternary interaction of water and the two blocks. Hydrated E−B has a much bigger χ than that of bulk EB and lamellar phase are known to be more stable (i.e., exist over a wider composition range) at higher χN. At intermediate concentration and independent of the molecular weight, E_mB_n copolymers have been found to generate lamellar phases that have periodicities that grow linearly with the water content. The lamellae swell up to a point where they start unbinding. The unbound membranes transform into a locally ordered sponge phase; the morphology of such a bicontinuous phase seems to be independent of the molecular weight. The sponge phase has a morphology that arises due to periodic modulations with short wavelength which are in counterphase with the next layer. Since both copolymers

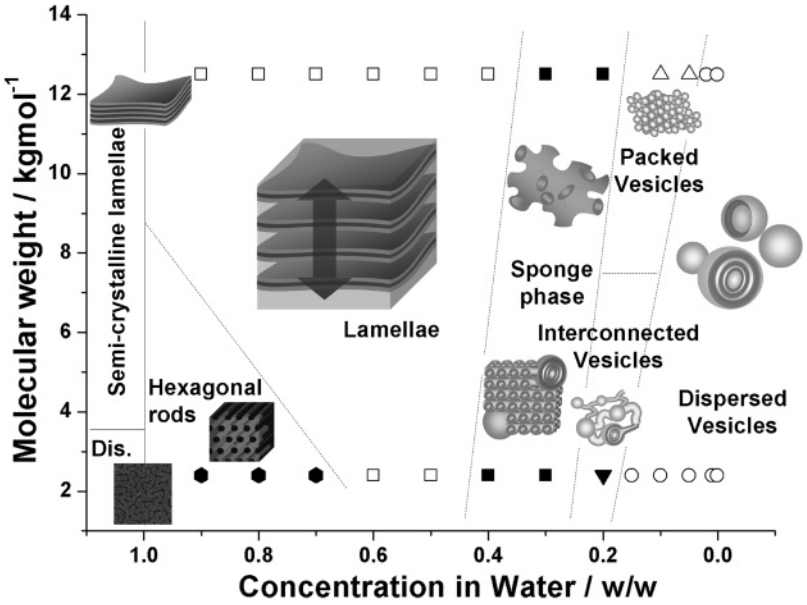

Figure 10. Isothermal phase diagrams of E_mB_n/water.

have a similar morphology, these undulations appear to be the result of the interfacial energy changes. Figure 4 shows that together with sponge phase there is substantial presence of multilamellar vesicles domains in the low molecular weight $E_{16}B_{22}$, whereas multilamellar vesicles have not been observed in high molecular weight $E_{115}B_{103}$. As indicated in Figure 5, the formation of multilamellar vesicles implies the presence of giant correlated fluctuations that are in counterphase with the next three or four layers. Such undulations are more likely to occur in more flexible membranes, and this is demonstrated by $E_{16}B_{22}$ assembling into a thinner membrane than $E_{115}B_{103}$ and having a much greater propensity to form multilamellar structures.

The evolution of the sponge phase into dispersed vesicles has also been found very different for the two block copolymers. The $E_{115}B_{103}$ sponge phase was observed to break up in gel clusters comprising close-packed unilamellar vesicles. Eventually, at very low concentrations, the vesicular clusters were observed to break up further into dispersed vesicles. In contrast, the lower molecular weight $E_{16}B_{22}$ forms multilamellar aggregates coexisting with the sponge phase, and in particular around 20% w/w, the sponge phase is made of multilamellar and unilamellar vesicles connected together by lamellar tubules.

At lower concentrations, both systems turn from gel to liquid and only vesicular aggregates have been observed, both multilamellar, already observed in gel state, and unilamellar. The two different populations can also be observed by DLS in dilute solution, and as the concentration $E_{16}B_{22}$ is reduced the multilamellar vesicles transform into unilamellar structures driven by osmotic pressure driven leakage.

These results suggest a strong dependency of the E_mB_n morphology on the water concentration. Both copolymers have a good tendency to generate amphiphilic membranes with hydrophobic thickness constant with respect to the concentration. These membranes arrange geometrically in morphologies that can sometimes hint at long-range order such as the sponge *Im*3*m* phase and show clear interconnected multilamellar vesicles and hexagonal-packed vesicles. These different morphologies suggest four different assembly regimes according to the copolymer concentration: lyotropic phases (hexagonal rods and lamellae), bicontinuous phases (sponge), vesicular gels (interconnected multilamellar vesicles and hexagonal-packed vesicles), and eventually isotropic vesicles dispersions (multilamellar and unilamellar). Simply mixing the copolymer with water leads to the formation of dispersed vesicles in both systems via a path-dependent sequence of phases; this strongly implies that unilamellar vesicles are an equilibrium phase whereas multilamellar vesicles are a long-lived metastable phase. Moreover, the vesicle size distribution and topology (single or multilamellar) observed is a result of the membranes morphological pathway from lamellae to dispersed vesicles. The structure in dilute solution is dominated by the membrane unbinding at much higher concentration and the evolution of membrane undulations sets the topology of the enclosed amphiphilic membranes.

Acknowledgment. The authors thank the ICI Strategic Technology Group for financial support and the contribution of Dr. Shao-Min Mai, who synthesized the block copolymer.

References and Notes

(1) Israelachivili, J.; Wennerstrom, H. *Nature (London)* **1996**, *379*, 219−225.
(2) Tanford, C. *Proc. Natl. Acad. Sci. U.S.A.* **1979**, *76*, 4175−4176.
(3) Israelachivili, J. N. *Intermolecular & Surface Forces*, 9th ed.; Elsevier Science: Amsterdam, 2002.
(4) Discher, B. M.; Won, Y.-Y.; Ege, D. S.; Lee, J. C.-M.; Bates, F. S.; Discher, D. E.; Hammer, D. A. *Science* **1999**, *284*, 1143−1146.
(5) Battaglia, G.; Ryan, A. J. *J. Am. Chem. Soc.* **2005**, *127*, 8757−8764.
(6) Paschalis, A.; Bjorn, L. *Amphiphilic Block Copolymers: Self-Assembly and Applications*; Elsevier Science Ltd.: Amsterdam, 2000.
(7) Hamley, I. W. *The Physics of Block Copolymers*; Oxford University Press: Oxford, 1998.
(8) Discher, D. E.; Eisenberg, A. *Science* **2002**, *297*, 967−973.
(9) Förster, S.; Zisenis, M.; Wenz, E.; Antonietti, M. *J. Chem. Phys.* **1996**, *104*, 9956−9970.
(10) Kabanov, A. V.; Bronich, T. K.; Kabanov, V. A.; Yu, K.; Eisenberg, A. *J. Am. Chem. Soc.* **1998**, *120*, 9941−9942.
(11) Dalhaimer, P.; Bermudez, H.; Discher, D. E. *J. Polym. Sci., Part B: Polym. Phys.* **2004**, *42*, 168−176.
(12) Antonietti, M.; Förster, S. *Adv. Mater.* **2003**, *15*, 1323−1333.
(13) Ghoroghchian, P. P.; Frail, P. R.; Susumu, K.; Blessington, D.; Brannan, A. K.; Bates, F. S.; Chance, B.; Hammer, D. A.; Therien, M. J. *Proc. Natl. Acad. Sci. U.S.A.* **2005**, *102*, 2922−2927.
(14) Stanish, I.; Lowy, D. A.; Hung, C.-W.; Singh, A. *Adv. Mater.* **2005**, *17*, 1194−1198.
(15) Hamley, I. W.; Mai, S.-M.; Ryan, A. J.; Fairclough, J. P. A.; Booth, C. *Phys. Chem. Chem. Phys.* **2001**, *3*, 2972−2980.
(16) Förster, S.; Berton, B.; Hentze, H.-P.; Kramer, E.; Antonietti, M.; Lindner, P. *Macromolecules* **2001**, *34*, 4610−4623.

(17) Booth, C.; Yu, G.-E.; Nace, V. M. In *Amphiphilic Block Copolymers: Self-Assembly and Applications*; Paschalis, A., Bjorn, L., Eds.; Elsevier Science Ltd.: Amsterdam, 2000.
(18) Bernheim-Groswasser, A.; Wachtel, E.; Talmon, Y. *Langmuir* **2000**, *16*, 4131−4140.
(19) Helfrich, W. *J. Phys: Condens. Matter* **1994**, *6*, A79−A92.
(20) Lipowsky, R. *Nature (London)* **1991**, *349*, 475−481.
(21) Demé, B.; Dubois, M.; Gulik-Krzywicki, T.; Zemb, T. *Langmuir* **2002**, *18*, 997−1004.
(22) Tiddy, G. J. T. *Phys. Rep.* **1980**, *57*, 1−46.
(23) Mutz, M.; Helfrich, W. *Phys. Rev. Lett.* **1989**, *62*, 2881−2884.
(24) Granek, R.; Cates, M. E. *Phys. Rev. A* **1992**, *46*, 3319−3334.
(25) Roux, D.; Codon, C.; Cates, M. E. *J. Phys. Chem.* **1992**, *96*, 4174−4187.
(26) Lipowsky, R.; Leibler, S. *Phys. Rev. Lett.* **1986**, *56*, 2541−2544.
(27) Leibler, S.; Lipowsky, R. *Phys. Rev. B* **1987**, *35*, 7004−7009.
(28) Goetz, R.; Helfrich, W. *J. Phys. II* **1996**, *6*, 215−223.
(29) Bermudez, H.; Brannan, A. K.; Hammer, D. A.; Bates, F. S.; Discher, D. E. *Macromolecules* **2002**, *35*, 8203−8208.
(30) Battaglia, G.; Ryan, A. J. *Nat. Mater.* **2005**, *4*, 869−876.
(31) Ryan, A. J.; Mai, S.-M.; Fairclough, J. P. A.; Hamley, I. W.; Booth, C. *Phys. Chem. Chem. Phys.* **2001**, *3*, 2961−2971.
(32) Cernik, R. J.; Barnes, P.; Greaves, G. N.; Rayment, T.; Ryan, A. J. *Appl. Crystallogr.* **2004**, *19*, 3−9.
(33) Ryan, A. J.; Fairclough, J. P. A.; Hamley, I. W.; Mai, S.-M.; Booth, C. *Macromolecules* **1997**, *30*, 1723−1727.
(34) Helfrich, W. In *Giant Vesicles*; Luisi, P. L., Walde, P., Eds.; John Wiley & Sons Ltd.: Chichester, 2000.
(35) Helfrich, W. *Eur. Phys. J. B* **1998**, *1*, 481−489.
(36) Auguste, F.; Douliez, J.-P.; Bellocq, A.-M.; Dufourc, E. J.; Gulik-Krzywicki, T. *Langmuir* **1997**, *13*, 666−672.
(37) Alexandridis, P.; Olsson, U.; Lindman, B. *Langmuir* **1997**, *13*, 23−34.
(38) Rummel, G.; Hardmeyer, A.; Widmer, C.; Chiu, M. L.; Nollert, P.; Locher, K. P.; Pedruzzi, I.; Landau, E. M.; Rosenbusch, J. P. *J. Struct. Biol.* **1998**, *121*, 82−91.

MA052108A